A FEASIBILITY STUDY ON THE USE OF A COINCIDENCE MASS SPECTROMETER TO DETERMINE LUNAR ATMOSPHERE CONSTITUENTS

Final Report

January 31, 1967

National Aeronautics and Space Administration

Contract No. NAS 9-4830

from

Southwest Center for Advanced Studies
Earth and Planetary Sciences Laboratory
Division of Atmospheric and Space Sciences

F. S. Johnson

Principal Investigator

A FEASIBILITY STUDY ON THE USE OF A COINCIDENCE MASS SPECTROMETER TO DETERMINE LUNAR ATMOSPHERE CONSTITUENTS

Summary

A Coincidence Mass Spectrometer built by Johnston Laboratories Inc. was procured by the Southwest Center for Advanced Studies for test and evaluation for suitability for adaptation for use on the lunar surface to make atmospheric measurements of residual lunar gases. Since the instrument has a unique means of discriminating against noise pulses by requiring that both the ion and the electron released in an ionization event be detected, it appears to have special merit for lunar measurements, where the gas pressures are exceedingly low and a good signal-to-noise ratio will be required to permit the measurement of minor constituents. In experimental evaluation, the instrument clearly has considerable merit. However, its full potential is limited by noise introduced by stray electrons from the electron beam and from modest sensitivity due to the requirement that no more than one ion be in flight in the drift tube at one time - the mass analysis is accomplished by measuring ion time-of-flight in a drift tube. Nevertheless, it seems probable that the instrument performance at very low pressure (below 10^{-12} torr) can be expected to at least equal, and probably better, that of any other type of instrument. Since the predicted performance at very low pressure for both this type instrument and other types involves extrapolation by two or more orders of magnitude, there is considerable uncertainty in this conclusion. This uncertainty can only be resolved by further development of several instruments that appear to be suited to lunar measurements, such as magnetic, quadrupole, and coincidence instruments, followed by comparative tests in a single system.

Introduction

As originally delivered, the instrument had an unduly high noise level which was recognized as due to stray electrons from the electron beam in the ion source. This was identified at JLI as due to scattering at one of the defining slits for the beam. In the fall of 1966, a new ion source involving the use of a saddle point lens instead of a slit was built at JLI, and this was installed on the instrument during the winter. Since that time, testing has proceeded on the revised instrument.

The Coincidence Mass Spectrometer (CMS) is a unique instrument that appears to have particular advantages for measurement of the lunar atmosphere. The lunar atmosphere is usually estimated to be very tenuous, in the neighborhood of 10^{-11} torr, although there is great uncertainty in this estimate, and the pressure could be considerably higher. Recognizing the fact that minor constituents of the lunar atmosphere could be important indicators of geologic conditions on the moon, it seems desirable to set a goal of measuring partial pressures as low as 10^{-15} torr. This must be accomplished under rather severe thermal conditions prevailing during the lunar day and night and in the presence of cosmic radiation without the shielding advantage of the geomagnetic field that reduces the high-energy particle radiation on laboratory instruments. The coincidence feature of the CMS provides a means of discrimination against noise that is not available in other instruments, and its method of analysis permits the simultaneous examination of the entire mass range rather than looking for one given mass at a time; these are the factors that suggest that the CMS might be the best instrument to analyze the lunar atmosphere.

To investigate the suitability of the CMS for making measurements of the lunar atmosphere, a laboratory instrument has been procured from Johnston Laboratories Inc. (JLI), Baltimore, Maryland. This instrument was delivered to the Southwest Center for Advanced Studies near the end of May, 1966. Since that time, the instrument has undergone intensive, though not complete, testing. Although some features of the instrument behavior still appear anomalous in some degree, its principal characteristics and limitations appear to have been well determined.

Instrument Description

The basic CMS is shown schematically in Figure 1. A very narrow well-collimated beam of electrons is produced by the electron gun; this beam disects the space between grids G_1 and G_2. A transverse electric field in this region causes the secondary electron produced by a gas ionization event to be accelerated toward the electron detector, while the corresponding ion is accelerated in the opposite direction. The ion passes through a field-free drift tube, and arrives at the ion detector a few microseconds after the electron reaches the electron detector. Neglecting the very short travel time of the electron, this time interval is directly proportional to the square root of the mass-to-charge ratio of the ion. These time intervals representing mass-to-charge ratios are measured and stored digitally by the data handling electronics. Thus, the instrument is not tuned to a single mass unit, but is prepared to accept signals from any mass unit at any time, except for dead times that arise in the logic during which no signals at all are accepted.

The logic functions of the CMS require that analysis proceed one ion at a time - it is not possible to operate with more than one ion simultaneously

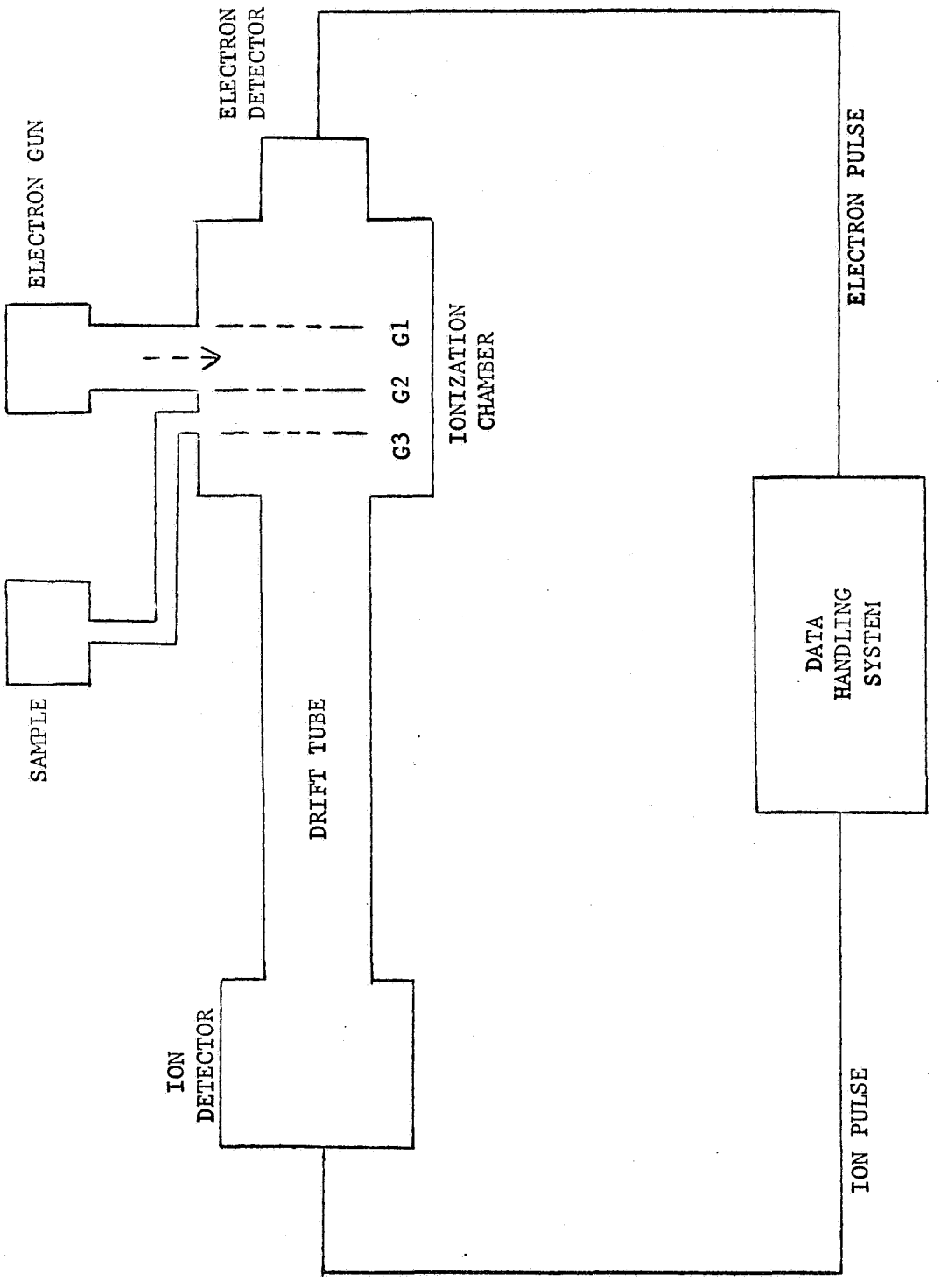

Figure 1. Schematic Representation of the Basic Coincidence Mass Spectrometer.

in flight through the spectrometer as it is with most other types of spectrometers. This limits the CMS to relatively low signal rates. The electron beam in the ionization source is correspondingly weak compared to that used in most other instruments.

The coincidence principle requires that a pair of correlated events occur before an ionization event can be recorded. For each ion that is collected, there must be a corresponding electron collected at the opposite detector. By use of this principle, the CMS is able to discriminate against noise pulses from the detectors. Noise occurs in the CMS only when pairs of noise pulses occur with such a relationship to one another that they are not distinguishable from signal pulses.

The mass discrimination accomplished by the CMS depends upon the accurate measurement of the difference in time of flight of ions of adjacent masses. The time of flight is

$$t_i = d\sqrt{\frac{m_i}{2 V e}} + \delta t_i \qquad (1)$$

where t_i is the time of flight of an ion of mass m_i, d is the length of the drift tube, V is the constant accelerating voltage, e is the charge on the ion, and δt_i depends upon the instrument parameters and represents the short drift time in the accelerating region. The δt_i are proportional to $\sqrt{m_i}$, so equation (1) can be written

$$t_i = k_1 \sqrt{m_i} \qquad (2)$$

and $k_1 \approx 10^{-6}$ for the CMS under evaluation (when a short drift tube is used), where t_i is expressed in seconds and m_i in atomic mass units. In

the CMS (see Figure 1), detection of an electron from an ionizing event starts a clock. The detection of an ion from the same event stops the clock, and in this way a measurement of t_i is accomplished.

The requirements on time resolution in order to resolve one atomic mass unit at mass m_i is

$$\Delta t_i = k_1\sqrt{m_i} - k_1\sqrt{m_i - 1}$$

$$= \frac{k_1\sqrt{m_i}}{2m_i} \qquad (3)$$

$$= \frac{10^{-6}}{2\sqrt{m_i}} \qquad \text{for the present instrument.}$$

This amounts to 2.5×10^{-8} sec (25 nanoseconds) for resolution of 1 amu at mass 400, or 5×10^{-8} sec (50 nanoseconds) at mass 100. The corresponding drift times are 20 and 10 μs. These values for the complete range of mass values up to 200 are shown in Figure 2. It should be emphasized that this only indicates the time resolution requirements; with adequate time resolution, the actual resolution of the instrument will be limited by such factors as thermal velocities in the source which in turn control the width of mass peaks. The full width of a mass peak m_i at half maximum is identified on a time scale as $\Delta\tau_i$, and $\Delta\tau_i = \Delta t_i$ at that mass which numerically equals the resolving power of spectrometer; at greater masses, $\Delta\tau_i > \Delta t_i$, and at lesser masses, $\Delta\tau_i < \Delta t_i$.

In a CMS without gated logic, there are four sequences of events that can produce error signals. These sequences are described below:

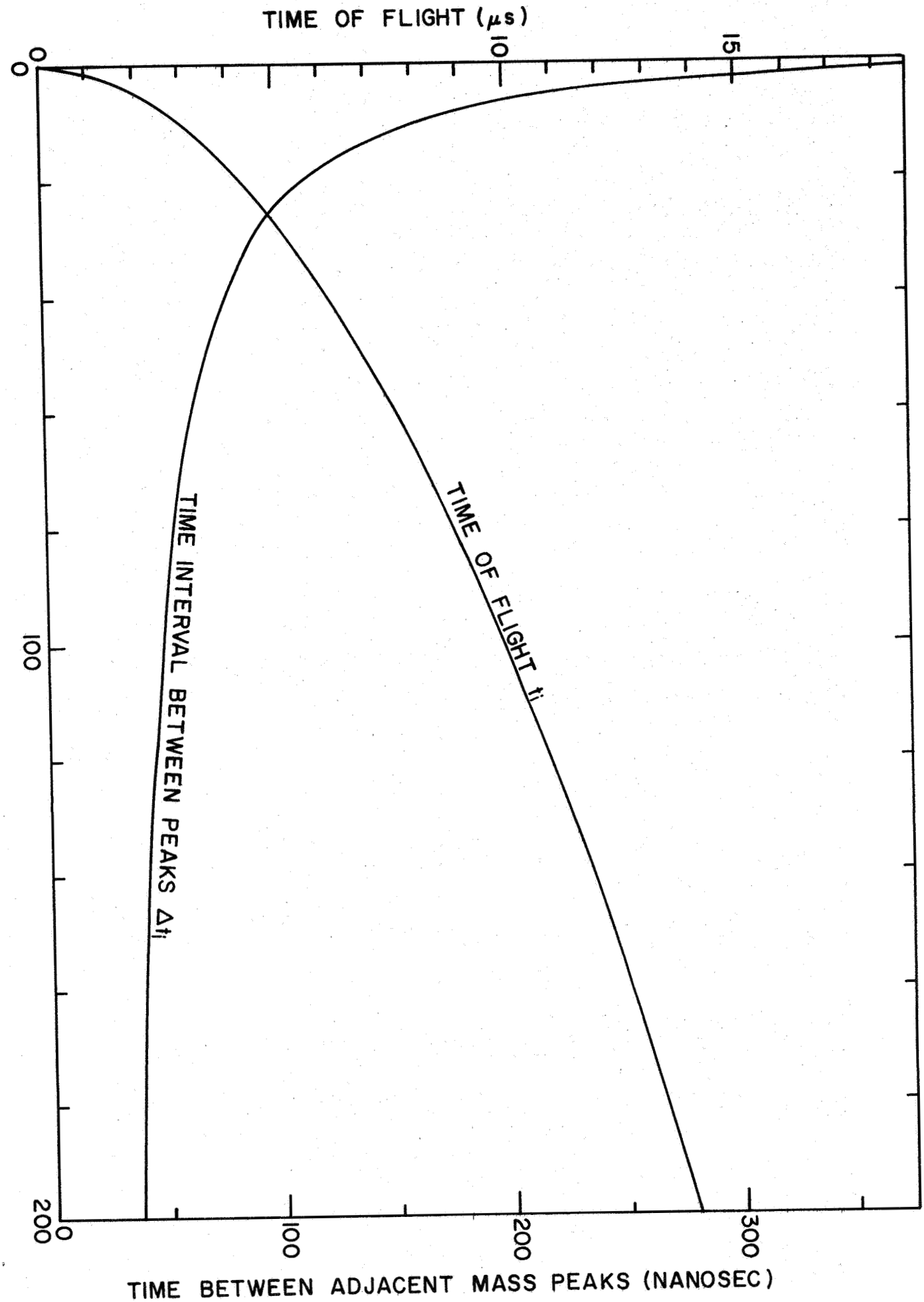
TIME OF FLIGHT (μs)
0
10
15
MASS (AMU)
0
100
200
TIME INTERVAL BETWEEN PEAKS Δti
TIME OF FLIGHT ti
0
100
200
300
TIME BETWEEN ADJACENT MASS PEAKS (NANOSEC)

FIGURE 2

1. A noise pulse from the electron detector followed by a noise pulse from the ion detector within the time limit imposed by the instrument.
2. An electron pulse from an actual ionization event followed by a noise pulse from the ion detector before the arrival of the ion.
3. An electron noise pulse followed by an ion pulse from an actual ionization event.
4. The ionization of a heavy particle followed by the ionization of a light particle within a time interval such that the ion of light mass can pass the heavier ion and produce an erroneous signal, or other incorrect associations of electrons and ions from different ionizing events.

Gated logic eliminates the noise sources of 3 and 4. Gated logic is a term that describes the controls necessary for eliminating certain noise signals. There are two separate gate functions, and these are described below:

1. When a pulse is received at the electron detector, the ionization of particles is stopped by turning off the electron beam for a period of 25 microseconds (75 microsecond gate is also available). Thus a noise pulse at the electron detector cannot be followed by a true ion pulse, since the electron beam is turned off immediately and no ions can be formed. Also, two ionization events

cannot take place separated by a short enough interval of time so as to cause erroneous pulses by incorrect association of pulses from the ion and electron detectors.

2. The path of the ions down the drift tube is blocked by a deflecting field until an electron pulse has been received, at which time the deflecting field is removed for 5 microseconds to permit the ion to pass. Thus if an electron from an ionization event is missed, the ion will be trapped and will not reach the ion detector.

The noise equations for the CMS are developed below. Let

N = true rate of ionization events per second

f_e = fraction of secondary electrons collected

N_e = true rate of detection of secondary electrons ($N_e = f_e N$)

N_s = rate of detection of stray electrons

N_n = noise rate in electron multiplier (and ion multiplier) when no particles are being detected

f_i = fraction of ions collected

The sources of noise described above contribute the number of noise counts indicated below within a time interval $\Delta\tau_i$ corresponding to the full width at half maximum of a mass peak at mass m_i.

1. Spurious noise arising from random noise pulses in ion and electron detectors and collection of stray electrons at the electron detector,

$$(N_n + N_s)\, N_n\, \Delta\tau_i \quad . \tag{4}$$

2. Noise caused by true electron events followed by noise pulses in the ion multiplier,

$$(f_e N)\ N_n\ \Delta\tau_i \quad . \tag{5}$$

If the ion from the ionization event is detected, a noise pulse from the ion detector at a later time will not contribute to noise, so this noise term decreases by a factor $(1-f_i)$ at the high end of the mass scale.

3. Noise caused by true ion detection events preceded by noise-triggered electron events,

$$(N_n + N_s)\ f_i\ N\Delta\tau_i \quad . \tag{6}$$

This term is eliminated with gated logic.

4. Noise caused two ionization events where the ion and electron that are detected are from different events,

$$(f_e\ N)\ (f_i\ N)\ \Delta\tau_i \quad . \tag{7}$$

This term is eliminated with gated logic.

The total noise counts that fall within the interval corresponding to the full width of a mass peak at half maximum are therefore

$$N_N = \Delta\tau_i \left[N_n^2 + N_s N_n + f_e N\ N_n + f_i N\ N_n + f_i N\ N_s + f_e f_i N^2 \right] \quad . \tag{8}$$

The signal rate is $f_e f_i N$, so the signal-to-noise ratio is

$$(S/N) = \frac{f_e\, f_i\, N}{\Delta\tau(N_n^2 + N_s N_n + f_e N\, N_n + f_i N\, N_n + f_i N\, N_s + f_e f_i N^2)} \qquad (9)$$

When gated logic is used, this reduces to

$$N_{NG} = \Delta\tau_i \left[N_n^2 + N_s N_n + f_e N\, N_n \right] \quad . \qquad (10)$$

and

$$(S/N) = \frac{f_e\, f_i\, N}{\Delta\tau_i\, N_n\, (N_n + N_s + f_e N)} \qquad (11)$$

The noise rate N_n in the electron multiplier is generally very low, probably below 10^{-1} sec^{-1}. The rate of ionization N is variable, depending upon pressure, and may range from 10^{-2} to 10^{5} sec^{-1}; the lower limit is set by the longest reasonable time to acquire a spectrum and the upper limit by the gated logic, which turns the electron beam off for 25 μs whenever an electron is detected. N_s is the rate of detection of stray electrons. In the original version of the instrument, these arose mainly from the electron beam, amounting to about 10^{-6} of the electron beam current. In the revised instrument, the stray electrons and count rates in general are strongly dependent upon the multiplier voltage adjustment - something that probably was also true with the original version but not thoroughly explored. When the multiplier voltage is 5000, which is the top of the meter range, the stray electrons do not exceed about 10^{-8} of the electron beam, as the stray electron count rate N_s does not exceed 10^{3} sec^{-1} when the beam current is 10^{-8} amp. If the multiplier voltage is turned up as far as possible - off scale

on the meter - the stray electron ratio increases to about 10^{-7}, as about 300 sec^{-1} are observed when the electron beam is 5×10^{-10} amp.

Without gated logic, the noise at high signal levels ($f_e f_i N > N_s$) would increase with increasing signal faster than the signal, leading to a decrease in signal-to-noise ratio with increasing signal levels. This decrease is caused by the noise contribution indicated in equation (7), which varies as N^2, while the signal varies directly with N.

The time interval $\Delta\tau_i$ corresponding to the width of a mass peak at half maximum varies with mass. The nature of the variation of $\Delta\tau_i$ with mass can easily be evaluated on the basis of the likelihood that the energy spread is the same for all masses. If the energy spread is V_o, the time difference across the peak will be approximately equal to the reversal time for an ion which is initially directed away from the ion detector, or

$$\Delta\tau_i = \frac{2}{E}\sqrt{\frac{2m_i V_o}{e}} \qquad (12)$$

where e is the electronic charge and E the electric field in the accelerating region. This can be written

$$\Delta\tau_i = k_2\sqrt{m_i} \quad , \qquad (13)$$

where k_2 is a constant that can be evaluated if the resolving power R of the instrument is known. When $m_i = R$, $\Delta\tau_i$ is equal to Δt_i, which is the time resolution required to separate adjacent mass peaks; this has been evaluated in Figure 2. The results are shown in Figure 3 for several values of resolving power. This indicates, for example, that the widths at half maximum of mass peaks in terms of a time scale vary from 25 ns at 100 amu to 36 ns at 200 amu when the resolving power of the instrument is 200. Since $\Delta\tau_i$ increases with mass, the signal-to-noise ratio decreases with increasing mass. This treatment has assumed implicity that noise pulses are uniformly

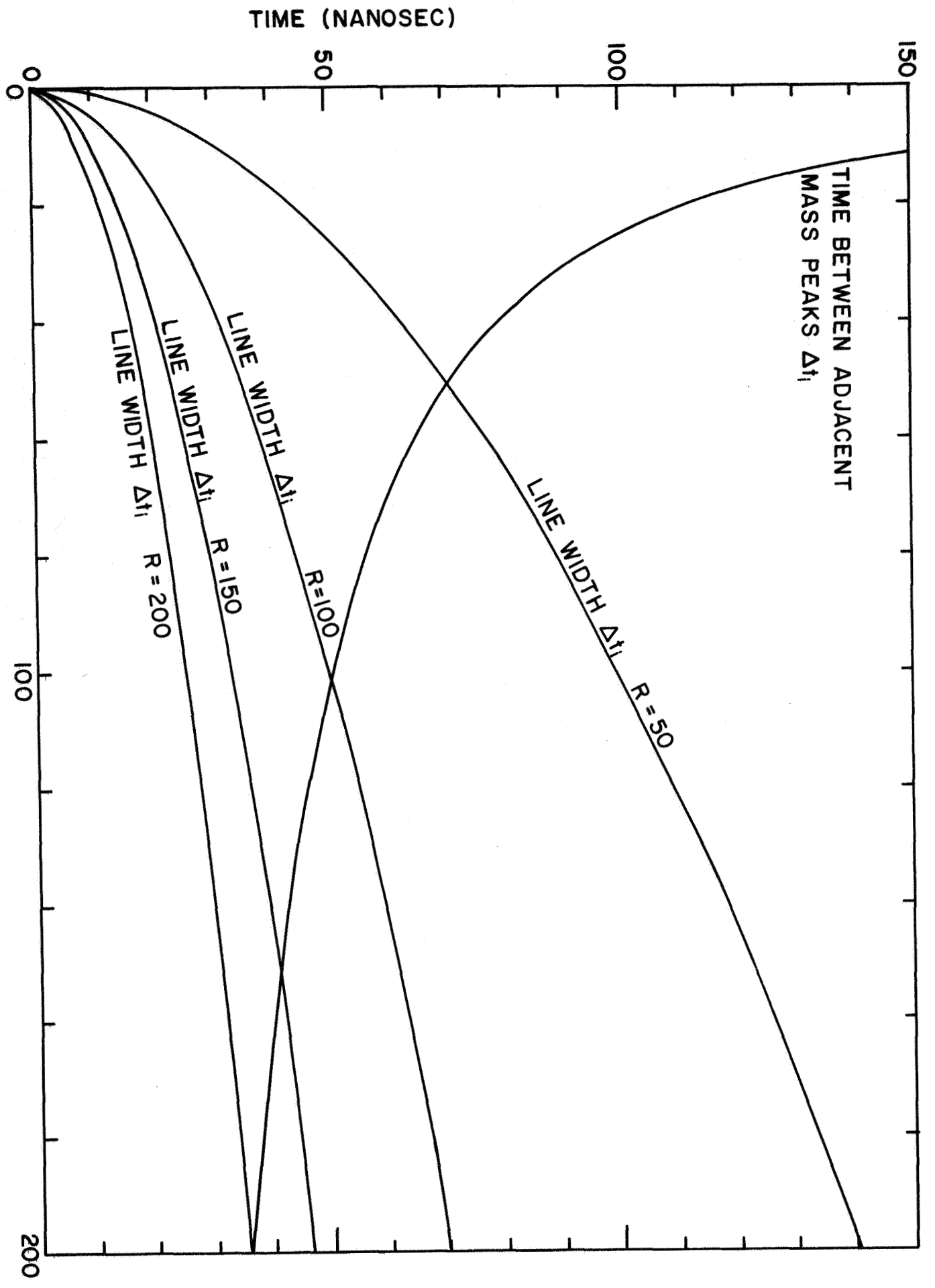
TIME (NANOSEC)
0
50
100
150
MASS (AMU)
0
100
200
TIME BETWEEN ADJACENT MASS PEAKS Δt_i
LINE WIDTH Δt_i R = 50
LINE WIDTH Δt_i R=100
LINE WIDTH Δt_i R = 150
LINE WIDTH Δt_i R = 200

FIGURE 3

distributed in time - an assumption that is probably justified with only minor reservations, such as that expressed following equation (5).

Other details of the CMS are discussed in Appendix 2, but the above discussion covers the essential factors governing its performance.

Performance of the Laboratory CMS

The specification on the vacuum system for the CMS was 5×10^{-9} torr, with bakeout to 400°C. This was not achieved with the original version of the instrument until the diffusion pump was replaced with an ion pump. After the new ion source was installed, leaks were never eliminated to the point of achieving that vacuum again, and it is felt that a new vacuum envelope would be required to get below 10^{-8} torr. Bakeout has been accomplished with temperatures at various parts of the instrument ranging from 280 to 400°C. The gold gaskets appear to show some tendency to leak after bakeout, and a better design might be found to reduce this. An originally present uncertainty introduced by an interaction between the CMS and the ionization pressure gage that is used to determine the pressure has been eliminated by relocating the vacuum gage. Originally when the CMS was turned on, the ionization gage apparently saw the drift tube potential and reacted to it in such a way that the pressure indication fell by about a factor of two. This apparently resulted from the ionization gage having been mounted physically too close to the drift tube.

The sensitivity in the original instrument was less than had been expected. With a beam current of 5×10^{-10} amp and a pressure of 10^{-6} torr, the signal rate was about 250 sec^{-1}. Extrapolating to obtain the expected count rate for a partial pressure of 10^{-15} torr - a reasonable objective for measurements on the moon - the count rate would be only

2.5×10^{-7} sec^{-1}. With the new ion source, a beam current of 9×10^{-9} amp at a pressure of 3×10^{-8} torr produces a signal rate of about 150 sec^{-1} when the multiplier voltage is 5000. This extrapolates to 5×10^{-6} sec^{-1} at 10^{-15} torr; the increase in sensitivity is just equal to the increase in electron beam current. It is thought that the beam current can be increased to 10^{-6} amp, or even possibly 10^{-5} amp. At 10^{-6} amp, the signal rate would be 5×10^{-4} sec^{-1}, still undesirably low even if the signal-to-noise ratio were adequate. It was anticipated that the extrapolated sensitivity at 10^{-15} torr would be about fifty times larger than this, based on information regarding the sensitivity of earlier CMS instruments. A quadrupole or other mass analyzer with an ion source capable of delivering 10^{-4} amp/torr - something that can be expected from a source utilizing a 3×10^{-4} amp beam of 80-volt electrons - should have a signal rate of 1 sec^{-1} at 10^{-15} torr. This would provide a signal-to-noise ratio of unity if the spurious count rate of a multiplier detector were 1 sec^{-1}. To provide for scanning of the spectrum over a mass range of about 100 with resolution near 100, the average count rate per mass unit would be about 10^{-2} sec^{-1}, or about ten times greater than is apparently to be expected from a CMS when the multiplier voltage is 5000 V. If the multiplier voltage is run up to the top of the range, the sensitivity of the CMS is increased by a factor of about twenty, so under these conditions the CMS performance might be expected to equal that of a quadrupole.

The resolution of the CMS is generally very good. With a long drift tube, a resolution of 350 was attained; this is significantly below the specification of 500, but is high enough for all foreseeable needs. With the normal drift tube, the resolution is not as high. A careful measurement of the width of the N_2 peak indicated a width at half maximum of 17 ns,

which, according to Figure 3, corresponds to a resolution of about 150, also ample for all recognized needs.

The signal-to-noise performance of the CMS is the most vital characteristic to evaluate, since it is in the area that the CMS has potential advantages over all other instruments. This can be predicted on the basis of equations (9) and (11), provided values are obtained for a number of operating characteristics of the instrument.

The ion and electron collection efficiencies are easily obtained by comparing the electron count rate $f_e N$, the ion count rate $f_i N$ (obtained with the gated logic off), and the coincidence rate $f_e f_i N$. This is indicated in Table 1, where data are shown for a multiplier voltage of 5000 V and a greater value which could not be read directly. Although there is considerable scatter in the determinations, it appears reasonable to accept $f_i = 0.13$ and $f_e = 0.04$ when the multiplier voltage is 5000 V, and $f_i = 0.25$ and $f_e = 0.4$ when the maximum multiplier voltage is used. These values can be changed some by changing some of the instrument adjustments, but they can be regarded as reasonably typical. The sensitivity of these factors to changes in operating voltage on the multiplier must be regarded as a disadvantage of the instrument. However, it affects principally the sensitivity - it should not affect the accuracy.

It turns out that the ion gate is only partially effective, and this must be taken into account in evaluating the signal-to-noise ratio. The gate efficiency can be evaluated by measuring the ion count rate with the logic off and with the gate closed (i.e., logic in test portion). Determinations are summarized in Table 2. Again, there is considerable scatter, but 3×10^{-3} appears to be a reasonable value; the value does not appear to be dependent upon the multiplier voltage. Because of this limitation of the gate efficiency, the signal-to-noise ratio must be evaluated by using equation

TABLE 1

Count Rates with 5000 Volts on Multiplier

Pressure (torr)	Beam Current (amp)	$f_e N$	$f_e f_i N$	f_i	$f_i N$	f_e
1.0×10^{-6}	4×10^{-9}	20,000	4,200	0.21	62,000	0.07
1.0×10^{-6}	5×10^{-10}	2,500	340	0.14	8,000	0.042
5.0×10^{-7}	5×10^{-9}	14,000	2,500	0.17	44,000	0.06
5.0×10^{-7}	5×10^{-10}	1,300	180	0.14	4,500	0.04
3.0×10^{-7}	9×10^{-9}	8,100	1,600	0.20	28,000	0.06
3.0×10^{-7}	5×10^{-9}	4,600	680	0.15	15,000	0.05
3.0×10^{-7}	5×10^{-10}	450	60	0.13	1,800	0.03
1.2×10^{-7}	9×10^{-9}	4,500	600	0.13	15,000	0.04
1.2×10^{-7}	5×10^{-9}	2,200	280	0.13	6,500	0.04
1.2×10^{-7}	5×10^{-10}	200	26	0.13	500	0.05
2.6×10^{-8}	9×10^{-9}	1,500	150	0.10	4,200	0.035
2.6×10^{-8}	5×10^{-9}	750	75	0.10	2,200	0.034
2.6×10^{-8}	5×10^{-10}	70	6.0	0.12	200	0.03

Count Rates with Maximum Voltage on Multiplier

Pressure	Beam Current	$f_e N$	$f_e f_i N$	f_i	$f_i N$	f_e
2.6×10^{-7}	5×10^{-9}	36,000	15,000	0.42	24,000	0.62
2.6×10^{-7}	5×10^{-10}	4,000	1,000	0.25	2,800	0.36
2.6×10^{-7}	5×10^{-11}	400	110	0.28	250	0.44
9.3×10^{-8}	9×10^{-9}	30,000	9,000	0.30	20,000	0.45
9.3×10^{-8}	5×10^{-9}	15,000	4,200	0.28	9,000	0.47
9.3×10^{-8}	5×10^{-10}	1,500	360	0.24	800	0.45
9.3×10^{-8}	5×10^{-11}	140	35	0.25	100	0.35
3.4×10^{-8}	1.5×10^{-8}	22,000	5,000	0.23	11,000	0.45
2.9×10^{-8}	9×10^{-9}	11,000	2,400	0.22	5,800	0.41
2.7×10^{-8}	5×10^{-9}	6,200	1,100	0.18	3,000	0.37
2.5×10^{-8}	5×10^{-10}	600	80	0.13	250	0.32
2.5×10^{-8}	5×10^{-11}	60	7	0.12	30	0.23

TABLE 2

Ion Gate Efficiency, Multiplier Voltage 5000 V

Pressure (torr)	Beam Current (amp)	Ion Count Rates		Efficiency
		Logic Off	Gate Closed	
1.0×10^{-6}	4×10^{-9}	62,000	150	2.5×10^{-3}
1.0×10^{-6}	5×10^{-10}	8,000	24	3.0×10^{-3}
5.0×10^{-7}	5×10^{-9}	44,000	120	2.7×10^{-3}
5.0×10^{-7}	5×10^{-10}	4,500	20	4.4×10^{-4}
2.0×10^{-7}	9×10^{-9}	28,000	70	2.5×10^{-3}
2.0×10^{-7}	5×10^{-9}	15,000	45	3.0×10^{-3}
2.0×10^{-7}	5×10^{-10}	1,800	6	3.0×10^{-3}
1.2×10^{-7}	9×10^{-9}	15,000	45	3.0×10^{-3}
1.2×10^{-7}	5×10^{-9}	6,500	20	3.1×10^{-3}
1.2×10^{-7}	5×10^{-10}	500	4	8.0×10^{-3}
2.6×10^{-8}	9×10^{-9}	4,200	8	1.9×10^{-3}
2.6×10^{-8}	5×10^{-9}	2,200	7	3.2×10^{-3}
2.6×10^{-8}	5×10^{-10}	200	2	10.0×10^{-3}

Ion Gate Efficiency, Maximum Multiplier Voltage

Pressure	Beam Current	Ion Count Rates		Efficiency
		Logic Off	Gate Closed	
2.6×10^{-7}	5×10^{-9}	24,000	50	2.1×10^{-3}
2.6×10^{-7}	5×10^{-10}	2,800	6	2.1×10^{-3}
2.6×10^{-7}	5×10^{-11}	250	3	1.2×10^{-3}
9.3×10^{-8}	9×10^{-9}	20,000	45	2.2×10^{-3}
9.3×10^{-8}	5×10^{-9}	9,000	25	2.8×10^{-3}
9.3×10^{-8}	5×10^{-10}	800	6	7.5×10^{-3}
9.3×10^{-8}	5×10^{-11}	100	3	30.0×10^{-3}
3.4×10^{-8}	1.5×10^{-8}	11,000	35	3.2×10^{-3}
2.9×10^{-8}	9×10^{-9}	5,800	15	2.6×10^{-3}
2.7×10^{-8}	5×10^{-9}	3,000	5	1.7×10^{-3}
2.5×10^{-8}	5×10^{-10}	250	4	16.0×10^{-3}
2.5×10^{-8}	5×10^{-11}	30	2	67.0×10^{-3}

(9) instead of equation (11), but with f_i in the denominator reduced by the factor 3×10^{-3}; f_i in the numerator should not be changed.

In the original version of the instrument, the electron count rate became constant as the pressure was reduced, due to stray electrons from the ionizing beam, and the stray electron ratio was evaluated as 3×10^{-6}. From Table 1 for multiplier voltage 5000 V, it can be seen that the electron count rate with the new source is 70 when the beam current is 5×10^{-10} amp or 3×10^{9} electrons sec^{-1}. Comparison of the electron count rate with that at higher pressures indicates that stray electrons do not contribute significantly to the count rate of 70, and it is estimated that about 30 stray electrons per second might escape notice. This indicates that the stray electron ratio must be no greater than 10^{-8}. The noise calculations for 5000 V multiplier voltage have been made on the assumption that the ratio is equal to 10^{-8}. When the maximum multiplier voltage is used and as the pressure is reduced, there is a clear leveling off of the electron count rate, and the stray electron ratio is about 10^{-7}. In view of the fact that the higher multiplier voltage increases the efficiency f_e of detecting electrons by a factor of 10, this determination indicates that the stray electron ratio for 5000 V multiplier voltage is probably very close to 10^{-8}.

The noise rate N_n of the multipliers is not known, but is clearly very small. For the calculations, a value of 10^{-1} has been assumed.

Figure 4 shows the results of calculations for 5000 V multiplier voltage and electron beam currents of 10^{-6} and 5×10^{-10} amp, calculated from equation (9) using the values given above, and using a value of 25 ns for $\Delta\tau$, which according to Figure 3 is appropriate to resolution 100 near mass 30. The dashed curves apply for no gated logic, and the solid curves apply with gated logic, for which f_i in the denominator of equation (9) is

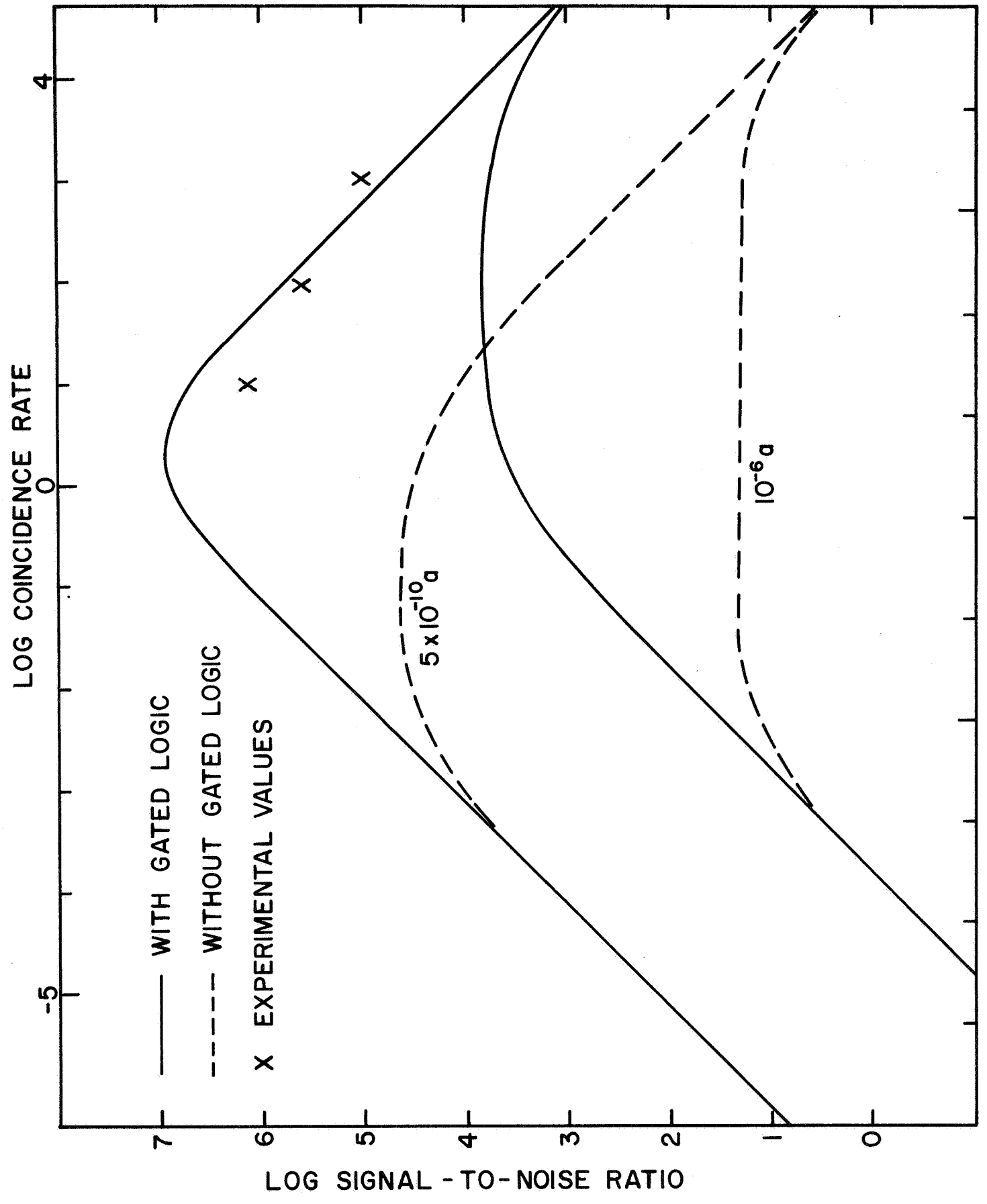
LOG COINCIDENCE RATE
4
0
-5
WITH GATED LOGIC
WITHOUT GATED LOGIC
X EXPERIMENTAL VALUES
5×10^{-10} a
10^{-6} a
7
6
5
4
3
2
1
0
-4
LOG SIGNAL - TO - NOISE RATIO
5
0
LOG IONIZATION RATE, 5000 V MULTIPLIER VOLTAGE

FIGURE 4

reduced by the factor 3×10^{-3} wherever it appears to take into account the fact that the ion gate is only partially effective. Three points are plotted - they are representative of experimentally determined signal-to-noise ratios with a beam current near 5×10^{-10} amp. The fit with the computed curves is surprisingly good, although the trend does not agree as well as one would like. Beam currents as large as 10^{-6} amp cannot be used in the present instrument, as the count rates get unacceptably large since the pressure cannot be reduced to sufficiently low values.

The signal-to-noise ratios indicated in Figure 4 for count rates below 1 sec^{-1} are not very reliable, as they depend upon N_n and N_s, both of which are poorly determined. The relatively low plateau on the curve for 10^{-6} amp with gated logic, about 10^4, is essentially set by N_s, and the sloping portion of the curves at very low count rates are governed by the product $N_n N_s$.

It was indicated earlier that a count rate of 5×10^{-4} sec^{-1} could be expected at 10^{-15} torr with a beam current of 10^{-6} amp. Figure 4 indicates that a signal-to-noise ratio just in excess of unity might be expected under these conditions. It was also mentioned earlier that the CMS is a factor of ten lower in sensitivity than the sensitivity predicted for a quadrupole working at unit signal-to-noise ratio. The similarity in signal-to-noise values suggests that the comparison is a valid one.

Signal-to-noise ratios to be expected at maximum multiplier voltage are shown in Figure 5, which is very similar to Figure 4. With the maximum multiplier voltage, a count rate of 10^{-2} sec^{-1} should be expected at 10^{-15} torr with a beam current of 10^{-6} amp. For this count rate, the signal-to-noise ratio, according to Figure 5, should be about 5. Thus performance is predicted to be slightly better than for a quadrupole.

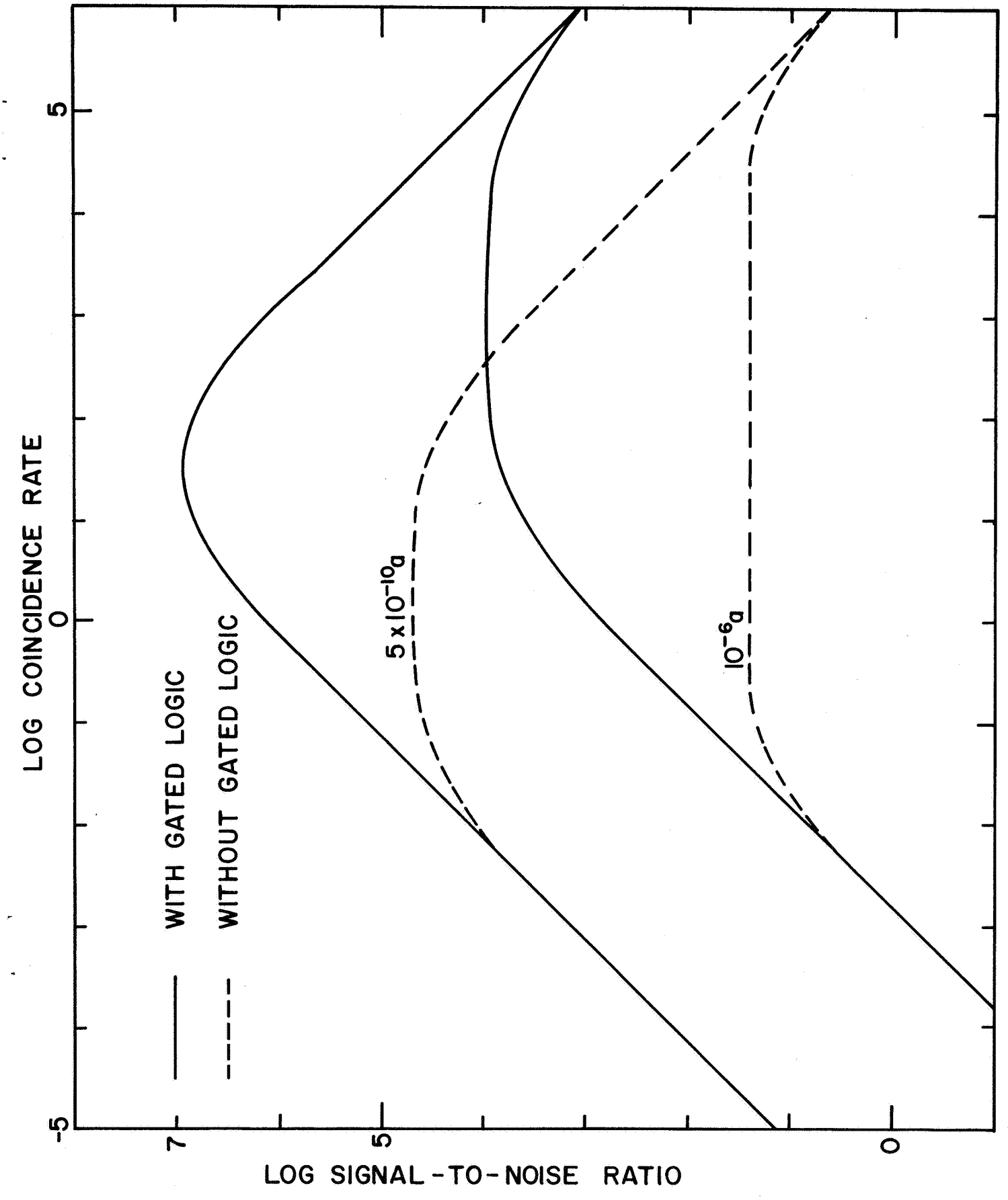
LOG COINCIDENCE RATE
5
0
-5
WITH GATED LOGIC
WITHOUT GATED LOGIC
5×10^{-10}a
10^{-6}a
7
5
0
LOG SIGNAL-TO-NOISE RATIO
5
0
-4
LOG IONIZATION RATE AT MAXIMUM MULTIPLIER VOLTAGE

FIGURE 5

It is clear that a major improvement in signal-to-noise could be achieved with a lesser ratio of stray electrons to beam electrons. It would be desirable to have a signal-to-noise ratio of 100, which would be achieved if the stray electron ratio were near 10^{-9}.

Prior to the initiation of this evaluation project, there was virtually no experience with CMS operation outside the plant of the manufacturer, JLI. Its operation at SCAS has convinced the operators that the CMS has considerable capability. However, it is also clear that additional development is needed to bring it to its full potential. Testing has not been carried out at the pressures below 10^{-10} torr where its advantages should show up the best. This instrument was designed for laboratory operation rather than for test at particularly low pressure, and considerable rebuilding and repackaging would be required to permit test at pressures below 10^{-10} torr.

Substantial questions still remain concerning the noise level at low pressures. The estimates made in extrapolating expected performance in this study may have been too conservative, and signal-to-noise performance could turn out to be much better than suggested here. The CMS sensitivity will apparently be comparable to that achievable in other instruments such as the quadrupole. However, predicted performance at 10^{-6} amp represents an extrapolation by over two orders of magnitude, and unexpected effects may well appear when such a substantial change is made in operating parameters. Laboratory operation and evaluation of performance at high beam currents could only be accomplished if the vacuum is improved by a corresponding factor, so as to keep the count rates within acceptable bounds.

The reliability of the present instrument has not been impressive. There has been a substantial number of component failures.

APPENDIX I

The Lunar Atmosphere

Although the lunar atmosphere is known to be exceedingly tenuous, knowledge of its composition should prove to be of considerable value from a geochemical viewpoint. The fact that it is very tenuous also makes it particularly susceptible to contamination from flight operations. Hence, it is important to make the observations at the earliest possible time. Owing to its extreme tenuosity, a very sensitive mass spectrometer will be needed to determine its composition.

The lunar atmosphere is known from optical measurements to be less dense than about 10^{-6} that of the earth's, which is not a very stringent upper limit. A search for free electrons has set a much lower limit. Occultation of radio stars has disclosed that the concentration of electron (and therefore of ions also) does not exceed 20 cm^{-3}. An earlier number, 10^{3}, has sometimes been combined with a 10^{-3} degree of ionization, corresponding roughly to the degree of ionization at the maximum in the earth's ionosphere, to give a neutral particle concentration of $<10^{6}$ particles cm^{-3}, or $<3 \times 10^{-14}$ atm., or $<2 \times 10^{-11}$ torr. Even this was an unrealistic limit, as ion loss by diffusion to the surface would proceed so fast in such an atmosphere as to make the degree of ionization much smaller than that at the ionization maximum in the earth's atmosphere. A realistic limit based on the 10^{3} ions cm^{-3} is about 3×10^{-9} torr, whereas the limit indicated by the newer number is 4×10^{-10} torr, which corresponds to a concentration of about 1.4×10^{7} particle cm^{-3}.

Although the extent of the contamination problem due to rocket exhaust is difficult to assess, some estimates can be made easily. At the time of lift off, the instrumentation will be exposed to a dynamic pressure of about 2×10^{-4} torr for about 20 s; so far as water vapor is concerned, this corresponds to exposure to very dry air. Moist air with dew point 20^{o}C has water-vapor partial pressure of 17 torr, so the water vapor environment during lift off corresponds to air with relative humidity of 10^{-3}%. The mass flow in the rocket exhaust is 52 kg s^{-1}, or about a ton in the 20 seconds required for the rocket to depart.

Only a small fraction of the rocket exhaust can be absorbed on the lunar surface and later released over a relatively long period of time. If the mass of absorbed gas at the landing side is W grams, and it is released with a time constant τ, the rate of release is $\frac{W}{\tau} e^{-t/\tau}$. 1 g s^{-1} of gas with molecular weight 20 moving with a velocity of 30 m s^{-1} gives rise to a particle concentration of 1.5×10^{9} cm^{-3}, or a contaminant pressure of 4×10^{-8} torr. The time dependent contaminant pressure is therefore $(4 \times 10^{-8} W_e^{-t/\tau})/\tau$. For $W = 10^{4}$ g (corresponding to 1% absorption of the rocket gas), this indicates that $p > 10^{-10}$ torr for 10 days if $\tau = 10^{6}$ s; $p > 10^{-9}$ torr for 1 day if $\tau = 10^{5}$ s; $p > 10^{-8}$ torr for a few hours if $\tau = 10^{4}$ s; and $p > 10^{-6}$ torr for a few minutes if $\tau = 10^{2}$ s. Therefore, if the rate of release is fairly rapid - characterized by a time constant of a small fraction of a day - then the concentration becomes small after a day or two; and if the rate of release is slow - characterized by a time constant of many days - then the contaminant gas concentration is low because of its slow rate of release. If one percent of the rocket exhaust is absorbed and released with a time constant of 10 days, the contaminant partial pressure could be in excess of 10^{-10} torr

for 10 days. If the time constant were 1 day, the contaminant partial pressure would be in excess of 10^{-9} torr for a day, but would drop below 10^{-10} torr in a few days. If the time constant were 10^4 sec., the pressure would fall below 10^{-10} torr in less than a day.

The astronaut will use water evaporation in his back pack for cooling, and this will release water vapor near the back of his neck at the rate of about 0.3 g s^{-1}. This will give rise to a vapor pressure of about 10^{-4} torr at 1 m. This could seriously interfere with attempts to measure the composition of gases released at drill holes, but the effect should not be important for instrumentation left behind on the lunar surface by the astronaut when he leaves.

The nature of the lunar surface as indicated by orbiter pictures suggests that a lot of gas has been released. Although much of this must have escaped, it is not unrealistic to expect that enough remains to measure. Some idea of typical release rates can be obtained by considering other planets. The CO_2 average release rate on earth over geologic time has been about 5×10^9 cm^{-2} s^{-1}, and on Mars, it has been about 5×10^6. The H_2O release rate on earth has been about 5×10^{10} cm^{-2} s^{-1}, and the argon release, about 2.4×10^6 cm^{-2} s^{-1}. The time constant for escape from an atmosphere is given by

$$\tau = \frac{H}{\frac{1}{\sqrt{2\pi}} \left(\frac{kT}{m}\right)^{\frac{1}{2}} (1 + y)e^{-y}} ,$$

where $y = \frac{mgr}{kT}$, $H = \frac{kT}{mg}$ is the scale height, m the molecular mass, g the acceleration of gravity, r the distance from the center of the planet, k the Boltzman constant, and T the temperature.

M	T	g	4 (km)	$\frac{mgr}{kT} = y$	H (km)	τ (sec)
1	1300	830	6920	5.35	1290	3.25×10^{4}
4	1300	830	6920	21.4	324	4.4×10^{10} (1.5×10^{3} yr)
16	1300	830	6920	85.5	81	3.6×10^{27} (10^{20} yr)
4	2000	830	6920	13.9	498	4.54×10^{5} (6 days)
16	400	166	1738	13.9	125	5.1×10^{5} (6 days)
40	400	166	1738	34.8	50	1.53×10^{16} (5×10^{8} yr)

Note that atomic oxygen escapes from the moon as readily as helium escapes from the earth (T, 5 times smaller; M, 4 times greater; escape energy, 20 times smaller). For thermal escape alone, argon and heavier gases could accumulate on the moon for periods of half a billion years and longer.

The accumulation time for helium in the earth's atmosphere is much longer than the escape time from the exosphere, because of the large reservoir in the lower atmosphere. The helium content of the exosphere is about $6 \times 10^{5} \times 5 \times 10^{7} = 3 \times 10^{13}$ atoms cm^{-2}. The helium content of the troposphere is $5 \times 10^{-6} \times 3 \times 10^{19} \times 8 \times 10^{5} = 1.2 \times 10^{20}$ atoms cm^{-2}, or 0.4×10^{7} greater than the exospheric content. This increases the time constant for escape to 0.7×10^{5} years for a situation where the exospheric temperature remains at $2000^{o}K$, or to 10^{6} years if the exospheric temperature is as high as $2000^{o}K$ only 7% of the time. The helium flow rate upwards at the base of the exosphere at $2000^{o}K$ is $H/\tau = 5 \times 10^{7}/4.5 \times 10^{5} = 100$ cm s^{-1}, and the rate of loss is $6 \times 10^{5} \times 100 = 6 \times 10^{7}$ atoms cm^{-2} s^{-1}. The rate of loss averaged over a solar cycle is less than one tenth this figure,

as the high rate of loss is maintained only for a relatively brief period near the maximum of the solar cycle. Such considerations are however not relevant on the moon.

APPENDIX II

Electrical Operation of the Coincidence Mass Spectrometer

A schematic drawing of the CMS is shown in Figure A1, and the controls for the various parts are discussed below. Figure A2 shows the internal and interface electrical connectors.

The ion source consists of an electron beam in the form of a thin sheet between and parallel to two grids. The grids carry positive and negative potentials so that any ion-electron pairs that are formed in the electron beam are drawn out of the source region. The grid potentials are independently adjustable with controls labeled "ion accelerator" and "electron beam deflector"; since the electron beam is bent by the field between the grids, the controls somewhat interact with one another and with the "electron gun deflector" control for the electron beam, which controls the beam deflection before it enters the region between the grids. The voltage applied to the ion accelerator can be monitored on the function test meter by turning the selector switch to the position IAX100; similarly, the electron beam deflector voltage is monitored at position EBX100, while the electron gun deflector voltage cannot be monitored. The beam current can be controlled manually or servo controlled by the beam current or the ion rate, and there are controls to set the prescribed current or ion rate; the servo selector switch is labeled servo, and the controls are labeled "manual, beam, and ion rate." The filament power for the electron beam can be turned off by an independent switch labeled "filament power." The filament power can be monitored on the function test meter by turning the selector switch to FPX1. The electron beam is collected at an electron trap, and the current is

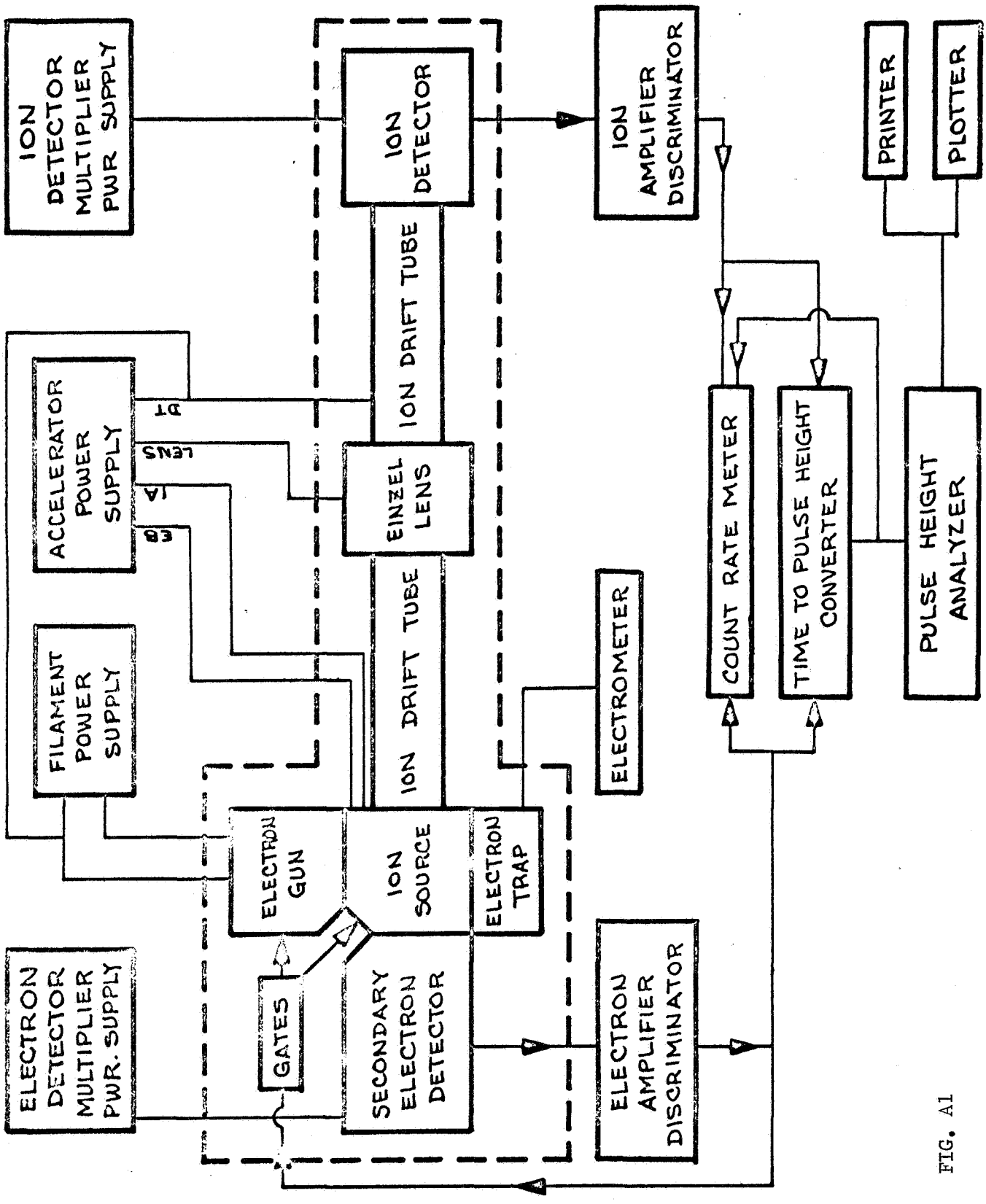
ION DETECTOR MULTIPLIER PWR SUPPLY
ION DETECTOR
ION AMPLIFIER DISCRIMINATOR
PRINTER
PLOTTER
ACCELERATOR POWER SUPPLY
DT
LENS
IA
EB
ION DRIFT TUBE
EINZEL LENS
COUNT RATE METER
TIME TO PULSE HEIGHT CONVERTER
PULSE HEIGHT ANALYZER
FILAMENT POWER SUPPLY
ION DRIFT TUBE
ELECTROMETER
ELECTRON GUN
ION SOURCE
ELECTRON TRAP
ELECTRON DETECTOR MULTIPLIER PWR. SUPPLY
GATES
SECONDARY ELECTRON DETECTOR
ELECTRON AMPLIFIER DISCRIMINATOR

FIG. A1

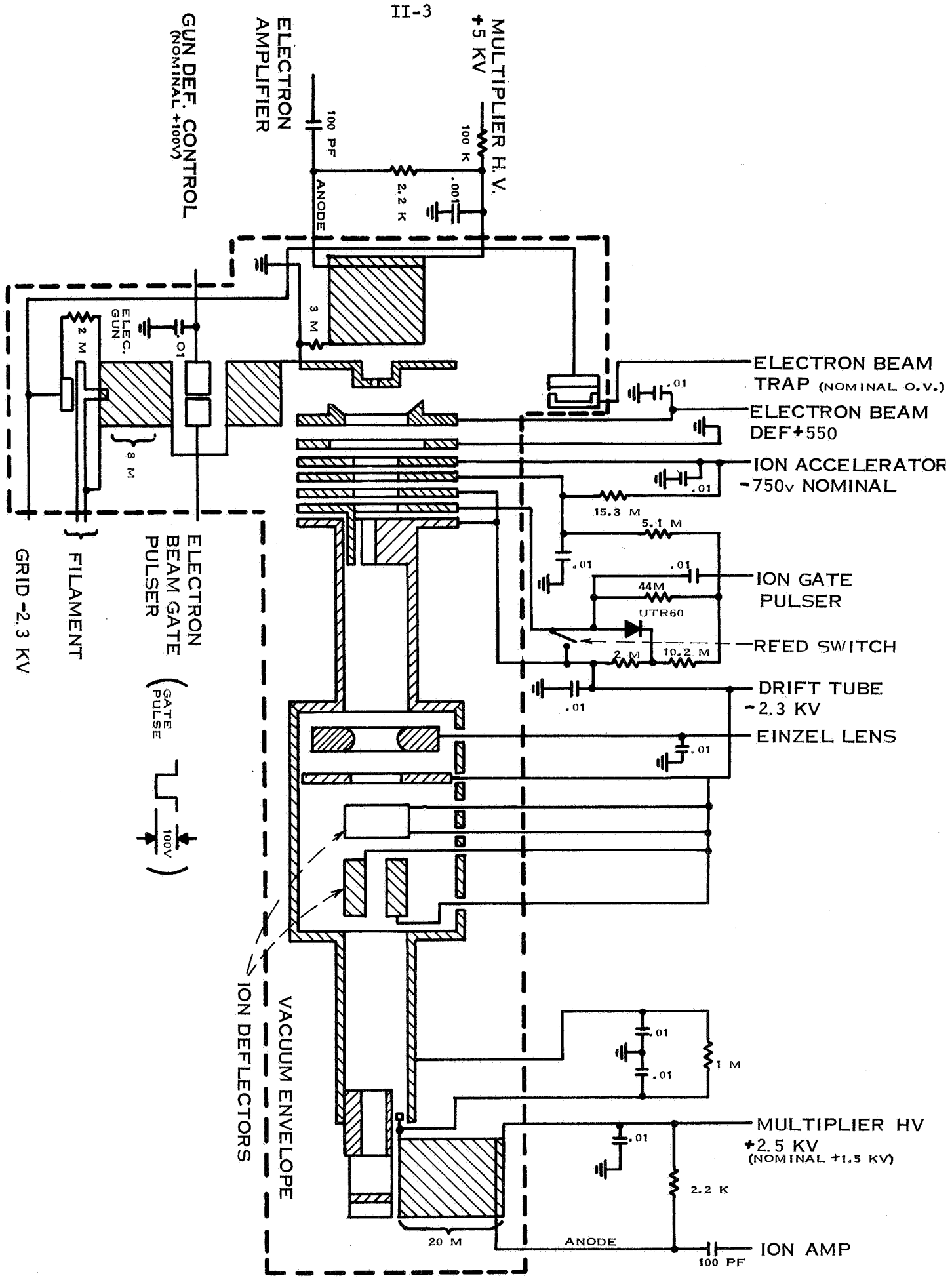

FIG. A2 COINCIDENCE MASS SPECTROMETER INTERNAL AND INTERFACE ELECTRICAL DIAGRAM

measured with an electrometer whose range is 10^{-12} to 10^{-7} amp. The electrometer output is displayed on a meter, and the electrometer of course becomes a part of the servo loop when the servo switch is in the "beam" position. To measure the electron beam current, the range control should first be turned to the "zero set" position and the "zero adjust" control should be used to zero the meter; then the selector switch can be turned to the appropriate range and the beam current read on the meter. There is a control grid in the electron gun so that the electron beam can be interrupted by the gated logic.

The electron detector consists of an electron multiplier, to which the required high voltage is supplied by a separate power supply. This power supply is controlled by a switch and a helipot to regulate the voltage; the voltage applied to the multiplier can be monitored by the function test meter when the selector switch is turned to the position EMX100. The multiplier is connected to an amplifier discriminator. The discriminator threshold is set by a potentimeter on the instrument control panel; there is also a switch to control the amplifier. This switch is labeled "electron amplifier" and the "discriminator threshold" adjustment is immediately above it. The dc voltage at the output of the first stage of the electron detector amplifier discriminator can be monitored on the function test meter by turning the selector switch to the position AEX.1. The output pulses from the amplifier discriminator have a length of about 400 ns. Output pulses from the amplifier discriminator connected to the electron detector go to 3 separate circuits - the gate pulse generator, the count rate meter, and the time-to-pulse-height converter.

The gate pulse generator is mounted at the rear of the spectrometer near the connection to the vacuum pump. When a pulse is received from the electron detector amplifier discriminator, the gate pulse generator generates two pulses, one to turn off the electron beam and one to open the gate for ions in the drift tube. The electron beam pulse has two possible lengths; the desired length is selected by means of a toggle switch on the pulse generator. In the down position, the pulse has a length of 25 μs (for use with the normal or short drift tube), and in the up position, about 75 μs (for use with the long drift tube). The pulse cuts off the electron beam for the corresponding period of time by means of a control grid. The ion gate pulse removes the voltage from deflecting plates that normally prohibit the drift of ions down the drift tube; on receipt of a pulse from the electron detector, the deflecting voltage is removed for 5 μs. Thus, this pulse generator provides the gated logic. There is a control on the control panel that permits the deactivation of this logic circuit. In the "off" position, the ion gate remains open continuously; in the "test" position, the ion gate remains closed continuously; the gating of the electron beam is not affected by the switch position. The voltage supplied to the gated logic circuit can be monitored on the function test meter by turning the selector switch to the position GLX10.

The count rate meter has two selector switches, one to select input from the electron detector, the ion detector, or the coincidence circuit. The other switch selects range.

The high voltage power supply provides high voltage for the electron beam, for the ion accelerator grid, for the Einzel lens, and for the drift

tube. The drift tube voltage and the ion accelerator voltages can both be monitored on the function test meter by turning the selectro switch to DTX100 and IAX100 respectively. The Einzel lens is an electrostatic focusing device to increase the proportion of ions passing down the drift tube that actually reaches the ion detector.

The ion detector consists of an electron multiplier, to which the required high voltage is supplied by a separate power supply. The power supply is controlled by a switch and a helipot; the voltage applied to the multiplier can be monitored by the function test meter by turning the selector switch to the position IMX100. The electron multiplier is connected to an amplifier discriminator. The discriminator level is set by a helipot on the instrument control panel, and there is also a switch to control the amplifier. The dc voltage at the output of the first stage of the ion detector amplifier discriminator can be monitored on the function test meter by turning the selector switch to the position AIX.1. The output pulses from the amplifier discriminator have a length of about 400 ns. Output pulses from the discriminator go both to the count rate meter and the time-to-pulse-height converter.

The low voltage power supply provides regulated voltages of -12 volts, +12 volts and +100 volts to operate the other electronic units. The $\pm$12 volt outputs can be monitored on the function meter by setting the selector switch at +LVX1 or -LVX1; and the +100 volt output can be monitored at GLX10. The two amplifier discriminators, the electrometer, the count rate meter, and the time-to-pulse-height converter operate on $\pm$12 volts. The electron-gate and ion-gate pulses operate on $\pm$12 and +60 volt. The filament power supply and the three high voltage power supplies operate from the 24 volts

available on the ±12 volt lines; these four supplies all use dc to ac inverters and employ almost identical voltage regulators and 30 kc oscillators.

The time-to-pulse-height converter requires two inputs and it provides one output. The sequence of events is (1) a pulse from the electron detector starts the cycle by activating a preset time delay circuit which is followed by a linear sawtooth generator whose rise time is also adjustable; (2) a pulse from the ion detector stops the sawtooth generator and holds the value which has been reached when the pulse was recieved; (3) a sample of the voltage reached by the sawtooth is taken and delivered to the output. The circuit then resets itself and awaits the next pulse from the electron detector. While performing its function, the converter will not accept pulses from the electron detector.

The start pulse is received at an input gate which is initially open; it triggers a delay sweep generator which generates a linear sawtooth voltage. The delay sweep generator sawtooth is applied simultaneously to two voltage comparators. The first has a low triggering level and triggers almost immediately, closing the input gate for the converter, thus rejecting any additional start pulses that might come along. The second comparator has its triggering level set with a helipot to give fine adjustment of the delay time to triggering; this starts the scan control. The scan control is a bi-stable multivibrator; it provides a pulse that resets the delay sweep generator, preparing it for the receipt of the next start pulse; it also triggers the scan sweep generator, which generates a highly linear sawtooth voltage. The scan sweep generator closely resembles the delay sweep generator, but it has only coarse adjustment of the scan time. The

scan sweep generator sawtooth is applied simultaneously to two voltage comparators; the first triggers an inhibit circuit almost immediately and keeps the input gate to the converter closed for the duration of the sweep; the second has a voltage level just below the maximum of the sawtooth, and it acts to reset the system if a stop pulse is not received during the sawtooth scan. The sawtooth is continuously applied to the output gate, which is normally closed. The stop pulse gate circuit consists of an AND gate and a one-shot monostable multivibrator. The AND gate require two input pulses, one of which is supplied by the scan generator for the duration of the scan sweep and the other of which is the stop pulse. When the two inputs are simultaneously present, the AND gate triggers the multivibrator. The first output from the multivibrator performs two functions. The first function is to trigger the level hold, which arrests the sawtooth scan and holds its value. The second function is to open the output gate after a suitable delay, allowing the sawtooth voltage attained at the time of the stop pulse to appear at the output. The width of the output pulse is determined by the one-shot multivibrator. The second output from the multivibrator resets the scan control, which in turn resets the scan sweep generator. This completes the cycle and the circuit is ready for another start pulse.

The scan sweep generator sawtooth waveform is generated by charging a capacitor with a constant current. When the generator is reset, the capacitor must be permitted to discharge, thus giving rise to an exponential decay of the sawtooth waveform. This presents no problem when the generator is reset by virtue of a stop pulse arrival, because the output pulse will have been obtained and the stop pulse gate closed, rejecting additional stop

pulses, before the exponential decay of the scan sweep generator waveform begins. If, alternatively, the upper level reset control resets the scan control, the slight delay in closing the stop pulse gate could permit a stop pulse to be effective in causing a sample of the generator output to be taken during its exponential decay. In this way, these meaningless pulses of random amplitude would contribute to background noise. To prevent this from occurring, the trigger pulse from the upper level reset is applied directly to the stop pulse gate, closing it, while the same pulse is delayed somewhat before being used to reset the scan control. This insures that the stop pulse gate is closed, to reject unwanted stop pulses, before the exponential decay of the sweep output is begun.

The output pulse from the time-to-pulse-height converter is analyzed by a commercial pulse height analyzer. Its operation is somewhat the inverse of the time-to-pulse-height converter. It will not accept additional pulses during its analysis cycle, which is generally longer than the time of flight of the ions that have generated the pulses. On this account, some signal pulses can be formed by the time-to-pulse-height converter but rejected by the pulse height analyzer because it is not ready for them.